Radiation Measurements 160 (2023) 106881

Contents lists available at ScienceDirect

Radiation Measurements

journal homepage: www.elsevier.com/locate/radmeas

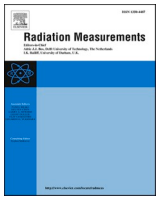

A model explaining the anomalous fading effect in thermoluminescence (TL)

J.L. Lawless [a], R. Chen [b,*], V. Pagonis [c]

[a] Redwood Scientific Incorporated, Pacifica, CA94044-4300, USA
[b] Raymond and Beverly Sackler School of Physics and Astronomy, Tel Aviv University, Tel Aviv, 69978, Israel
[c] Physics Department, McDaniel College, Westminster, MD21157, USA

ARTICLE INFO

Keywords:
Thermoluminescence (TL)
Anomalous fading
Simulations
Energy-level model

ABSTRACT

An energy-level model consisting of an electron trap, a hole trap and a hole recombination center is proposed to explain the anomalous-fading effect of thermoluminescence which has been observed in several materials. The present model is related to a thermoluminescence glow-curve consisting of two peaks. The relevant set of coupled differential equations is considered and a set of the relevant parameters is chosen. The equations are solved both by making plausible analytical approximations and numerically by using a Matlab solver; the results of the two approaches are in very good agreement. The simulated sample is excited at 100K and then held at room temperature or lower for different lengths of time before simulating the heating stage. It is found that as expected, the low-temperature peak at ~400K decays very quickly and quite anomalously, the high-temperature peak at ~570K is also fading much faster than expected for a peak occurring at this temperature. The dependence on the fading temperature, an effect which has been found in some materials is also demonstrated in the simulations. The numerical simulations and the analytical approximations can explain these results and show why this decoupling between the peak temperature and the fading takes place.

1. Introduction

Normal fading of a thermoluminescence (TL) signal is the effect of reduction of the expected TL signal when the sample is held at a temperature somewhat lower than that of the TL peak. The reason for this decay is the thermal release of trapped carriers and their subsequent recombination with opposite-sign carriers, all prior to the heating of the previously irradiated sample. An important condition for this normal fading is that the sample is held between the times of excitation and heating at a temperature rather close to that of the peak so that the thermal release of carriers from the relevant trap is quite fast. Normally, one does not expect such decay when the sample is held following the excitation at a temperature significantly lower than that of the peak. Several researchers found, however, that with certain TL materials, the signal decays quite fast when the sample is held at significantly lower temperatures. Putting it in a slightly different way, it was found that in these anomalous cases, the decay was much faster than expected for the effective trapping parameters determined from the shape or other properties of the TL peak in hand. The effect was termed "anomalous" or "abnormal" fading.

The first report of anomalous fading was given by Bull and Garlick (1950) for UV excited TL in diamonds. Two peaks at 400 and 520K were found to yield lower light levels following 6 h storage at 90K. Hoogenstraaten (1958) reported the decay of TL following rather short holding times at low temperature in ZnS samples doped with Cu, Co and Cl and explained it as being due to quantum mechanical tunneling of electrons from traps to holes in recombination centers. Schulman et al. (1969) reported the effect in CaF_2:Mn. A similar effect was found by Kieffer et al. (1971) in organic glasses. It is worth noting that in the results mentioned so far, no temperature dependence of the anomalous fading was reported.

Wintle (1973, 1977) has found the effect in various minerals at different temperatures and considered the implications with regards to the dating of archaeological samples. Wintle has suggested three alternative possibilities to explain anomalous fading: (a) defect diffusion which allows a non-radiative escape of trapped electrons when the diffusing defect encounters a trapping site; (b) direct transfer of an electron from a trap to an adjacent center as previously suggested by Garlick and Robinson (1972); (c) reduction in the number of effective recombination centers with time. These points have been further

* Corresponding author.
E-mail address: chenr@tau.ac.il (R. Chen).

https://doi.org/10.1016/j.radmeas.2022.106881
Received 10 October 2022; Received in revised form 14 November 2022; Accepted 17 November 2022
Available online 25 November 2022

considered by Jaek et al. (2007) who suggested that anomalous fading may not be explained by tunneling in some cases and maintained that other processes, in particular ionic processes may be the cause of the effect. It should be mentioned that the anomalous fading in feldspars described by Wintle is temperature dependent.

Visocekas et al. (1983) have studied the afterglow in $CaSO_4$:Dy and shown that after the initial irradiation, a weak afterglow is observed for a long period of time, with the same emission spectrum as the following TL. The peak used for dosimetry at 250 °C decayed with time practically independently of the temperature when the sample was held at temperatures between 80K and room temperature (RT). Their explanation was that the afterglow and anomalous fading in this material results from a quantum mechanical tunneling effect. Stoneham and Winter (1988) and Bowman (1988) communicated on the effect in majolica in the context of authenticity testing in archaeology.

A number of groups have investigated the anomalous fading in feldspars: Visocekas (2000), Meisl and Huntley (2005), Pagonis et al. (2012), Guérin and Visocekas (2015), Riedesel et al. (2021), Polymeris et al. (2022) and Devi et al. (2022). Kumar et al. (2022) considered the possibility that hole instability causes anomalous fading in feldspars. Different types of apatites have also exhibited the effect: Kitis et al. (2006), Tsirliganis et al. (2007), Sfampa et al. (2014), Polymeris et al. (2018). Comprehensive discussions on the existing models of anomalous fading have been given by Pagonis (2019, 2021). In a rather recent paper, Bringuier (2020) explains anomalous fading of TL in granitic feldspar as being due to a slight crystallographic disorder which enhances the decay of the TL signal.

Chen and Hag-Yahya (1997) have offered a possible model which included an electron trap and three recombination centers, one radiative and two non-radiative. The competition of the non-radiative centers causes the radiative peak to be narrow and therefore it yields an effective activation energy and a frequency factor which are much higher than the real ones. As a result, when one expects very long decay time of the signal, one gets much shorter decay time according to the real parameters. The authors term this kind of anomalous fading a normal fading in disguise.

In the present work we provide a rather simple alterative model that may explain temperature-dependent anomalous fading. We utilize a previous model (Chen et al., 2008; Lawless et al., 2021) developed for explaining effects of duplicitous TL peaks and of inability of exciting TL peaks in certain low temperature ranges. The model, explained in detail below, includes the possibility of thermal release of holes from hole traps in addition to the thermal release of electrons from their respective traps. The model bears some resemblance to the Schön-Klasens model (Schön, 1942; Klasens, 1946) in which the TL process includes both the thermal release of electrons into the conduction band and holes into the valence band. The possibility of having simultaneous release of electrons and holes from their respective traps has further been mentioned in the literature (e.g. McKeever et al., 1985; Mandowski, 2005). We show, using both results of numerical simulations and a theory with appropriate assumptions about the relevant parameters and approximations, that fading may occur at relatively low temperatures, for example, a peak occurring at 560K (287 °C) can fade significantly if the sample is held at room temperature for ~24 h.

2. The model

The proposed energy-level diagram is shown in Fig. 1. We consider an electron trap with concentration N (cm^{-3}) and instantaneous occupancy n (cm^{-3}), activation energy E (eV), and frequency factor s (s^{-1}). The transition-probability coefficient from the conduction band into the trap is denoted by A_n (cm^3s^{-1}). We also consider a hole trap with concentration M_2 (cm^{-3}) and instantaneous occupancy of m_2 (cm^{-3}), activation energy of releasing holes into the valence band E_{m2} (eV), frequency factor s_{m2} (s^{-1}) and hole trapping-probability coefficient B_2 (cm^3s^{-1}). We assume that recombination of free electrons with holes in

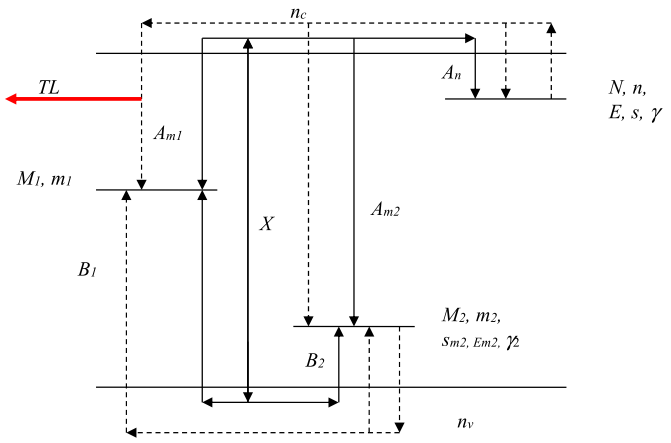

Fig. 1. Energy-level diagram of the model explaining the anomalous-fading effect. N is the electron trap, M_1 is the hole center and M_2 is the hole trap. The other parameters are defined in the text. Transitions taking place during excitation are shown in solid lines and transitions occurring during heating in dashed lines.

traps is allowed, and the probability coefficient is denoted by A_{m2} (cm^3s^{-1}). The recombination center concentration is M_1 (cm^{-3}) with instantaneous hole concentration of m_1 (cm^{-3}); the probability coefficient of holes from the valence band to get into the center is B_1 (cm^3s^{-1}) and the probability coefficient of recombination of electrons from the conduction band with holes in the luminescent center is A_{m1} (cm^3s^{-1}). The concentration of electrons in the conduction band is denoted by n_c (cm^{-3}) and that of the holes in the valence band is n_v (cm^{-3}). The rate of production of electron-hole pairs by the irradiation is X ($cm^{-3}s^{-1}$) which is proportional to the excitation dose rate, and the total absorbed dose is therefore proportional to the total concentration of pairs produced, namely, $D = X{\cdot}t_D$ (cm^{-3}) where t_D (s) is the excitation time.

The set of simultaneous differential equations governing the relevant processes is

$$\frac{dn}{dt} = A_n(N-n)n_c - n\gamma, \tag{1}$$

$$\frac{dm_1}{dt} = B_1(M_1-m_1)n_v - A_{m1}m_1n_c, \tag{2}$$

$$\frac{dm_2}{dt} = B_2(M_2-m_2)n_v - A_{m2}m_2n_c - m_2\gamma_{m2}, \tag{3}$$

$$\frac{dn_c}{dt} = X - A_n(N-n)n_c - A_{m2}m_2n_c - A_{m1}m_1n_c + n\gamma, \tag{4}$$

$$\frac{dn_v}{dt} = X - B_1(M_1-m_1)n_v - B_2(M_2-m_2)n_v + m_2\gamma_{m2}, \tag{5}$$

where

$$\gamma = s\exp(-E/kT), \tag{6}$$

$$\gamma_{m2} = s_{m2}\exp(-E_{m2}/kT). \tag{7}$$

We will assume that only recombination with the first center is radiative. Thus, the intensity, in units of photons emitted per unit volume per unit time ($cm^{-3}s^{-1}$) of emitted TL is given by

$$I = A_{m1}m_1n_c. \tag{8}$$

3. Theory

For the conditions of our simulations (see Section 4), the following assumptions are well justified,

$$m_1 \ll M_1 \quad and \quad m_2 \ll M_2. \tag{9}$$

Under these assumptions, Eq. (5) shows that the lifetime of free holes is $1/(B_1M_1+B_2M_2)$. For the condition of the simulation, this is 10^{-12}s. This is much shorter than any time scale for irradiation, fading, or heating. The lifetime for free electrons is similarly short. Consequently, n_c and n_v will be small and the quasi-steady approximation applies,

$$n_c = \frac{X + n\gamma}{A_n(N-n) + A_{m2}m_2 + A_{m1}m_1}, \tag{10}$$

$$n_v = \frac{X + m_2\gamma_{m2}}{B_1M_1 + B_2M_2}. \tag{11}$$

In this case, the governing equations (1)–(3) reduce to

$$\frac{dn}{dt} = \frac{A_n(N-n)}{A_n(N-n) + A_{m2}m_2 + A_{m1}m_1}X - \frac{A_{m2}m_2 + A_{m1}m_1}{A_n(N-n) + A_{m2}m_2 + A_{m1}m_1}n\gamma, \tag{12}$$

$$\frac{dm_1}{dt} = \frac{B_1M_1}{B_1M_1 + B_2M_2}(X + m_2\gamma_{m2}) - \frac{A_{m1}m_1}{A_n(N-n) + A_{m2}m_2 + A_{m1}m_1}(X + n\gamma), \tag{13}$$

$$\frac{dm_2}{dt} = \frac{B_2M_2}{B_1M_1 + B_2M_2}X - \frac{A_{m2}m_2}{A_n(N-n) + A_{m2}m_2 + A_{m1}m_1}(X + n\gamma) - \frac{B_1M_1}{B_1M_1 + B_2M_2}m_2\gamma_{m2}. \tag{14}$$

Each of the terms in Eqs. 12–14 has clear physical meaning. For example, from Eq. (13) which involves m_1, $(X + m_2\gamma_{m2})$ is the total rate at which free holes are created, X by irradiation and $m_2\gamma_{m2}$ by thermal release from M_2. The term $B_1M_1/(B_1M_1+B_2M_2)$ is the fraction of those holes that are recaptured by m_1.

As initial conditions before irradiation, we assume that all traps, bands and centers are empty: $n = m_1 = m_2 = n_c = n_v = 0$. Charge conservation then requires $n + n_c = m_1+m_2+n_v$ all along. When the quasi-steady approximation applies, the lifetimes of free electrons and holes are very short and the populations of free electrons and holes as given by Eqs. 10 and 11 become small. Consequently, $n_c << n$ and $n_v << m_1+m_2$. Thus, charge conservation simplifies to

$$n = m_1 + m_2. \tag{15}$$

Governing equations 12–15 will be the basis for the following sections which analyze irradiation, fading and heating and their effect on the two TL peaks.

3.1. Irradiation at low temperature

For irradiation at low temperature, terms involving γ or γ_{m2} can be neglected. In this case, Eqs. 12–14 simplify to

$$\frac{dn}{dt} = \frac{A_n(N-n)}{A_n(N-n) + A_{m2}m_2 + A_{m1}m_1}X, \tag{16}$$

$$\frac{dm_1}{dt} = \frac{B_1M_1}{B_1M_1 + B_2M_2}X - \frac{A_{m1}m_1}{A_n(N-n) + A_{m2}m_2 + A_{m1}m_1}X, \tag{17}$$

$$\frac{dm_2}{dt} = \frac{B_2M_2}{B_1M_1 + B_2M_2}X - \frac{A_{m2}m_2}{A_n(N-n) + A_{m2}m_2 + A_{m1}m_1}X. \tag{18}$$

Each of the terms here have clear physical significance. For example, the first term on the right in Eq. (18); X is the rate at which free holes are created and $B_2M_2/(B_1M_1+B_2M_2)$ is the fraction of those free holes which are captured by M_2 and therefore adding to the concentration of the center, m_2. X is also the rate at which free electrons are created and, in the second term on the right in Eq. (18), $A_{m2}m_2/[A_n(N\text{-}n)+A_{m2}m_2+A_{m1}m_1]$ is the fraction of those free electrons which end up recombining with m_2 and therefore reducing the concentration of center m_2.

We have earlier assumed that the applied dose would be low enough that Eq. (9) applied. To simplify the equations, we will here further assume that the dose is low enough that

$$A_{m1}m_1 + A_{m2}m_2 \ll A_nN \quad and \quad n \ll N. \tag{19}$$

Note that low dose assumptions Eq. (19) implies that the rate of trapping or retrapping of free electrons into n will be much larger than the rate of recombination of free electrons with either trap. Using Eq. (19), Eqs. 16–18 can be immediately integrated to obtain

$$n_a = D, \tag{20}$$

$$m_{1a} = \frac{B_1M_1}{B_1M_1 + B_2M_2}D, \tag{21}$$

$$m_{2a} = \frac{B_2M_2}{B_1M_1 + B_2M_2}D, \tag{22}$$

where the subscript a is used to indicate that these values are at the end of irradiation and D is the dose,

$$D = \int_0^t X dt'. \tag{23}$$

In later sections, we will assume that

$$B_1M_1 \ll B_2M_2. \tag{24}$$

Combined with Eqs. 21 and 22, Eq. (24) implies that, after irradiation, $m_{1a} << m_{2a}$. This will help to simplify the math.

In sum, subject to the low-dose assumption, Eq. (19), the trap and center populations at the end of irradiation are given by Eqs. 20–22. Note that under the described conditions, the results depend on the total dose applied and one does not expect dose-rate effects.

3.2. Decay at mid-temperatures

After irradiation, we allow the populations to decay at a temperature that is high enough so that γ is large enough to enable the release of electrons, but at still low enough temperature that γ_{m2} is negligible. With $X = 0$ and γ_{m2} negligible, Eqs. 12–14 reduce to

$$\frac{dn}{dt} = -\frac{A_{m2}m_2 + A_{m1}m_1}{A_n(N-n) + A_{m2}m_2 + A_{m1}m_1}n\gamma, \tag{25}$$

$$\frac{dm_1}{dt} = -\frac{A_{m1}m_1}{A_n(N-n) + A_{m2}m_2 + A_{m1}m_1}n\gamma, \tag{26}$$

$$\frac{dm_2}{dt} = -\frac{A_{m2}m_2}{A_n(N-n) + A_{m2}m_2 + A_{m1}m_1}n\gamma. \tag{27}$$

These equations are subject to the initial conditions, Eqs. 20–22.

We can learn about the relative speed at which m_1 and m_2 decay by taking the ratio of Eq. (26) to Eq. (27) to find

$$\frac{d\ln(m_1)}{d\ln(m_2)} = \frac{A_{m1}}{A_{m2}}. \tag{28}$$

To both simplify the equations and to obtain the anomalous behavior that we want, we will assume

$$A_{m1} \gg A_{m2}. \tag{29}$$

The combination of Eqs. (28) and (29) means that, as decay proceeds, m_1 will experience a large fractional decline before there is any significant fractional reduction in the population m_2. Thus, for much of the decay of m_1, we can consider m_2 to be approximately constant. To proceed, let us simplify Eq. (26) using Eq. (19) to find

$$\frac{dm_1}{dt} = -\frac{A_{m1}m_1}{A_nN}n\gamma. \tag{30}$$

From charge conservation, $n = m_1+m_2$. Since, during the decay of m_1,

the value of m_2 is approximately unchanged from its initial value, m_{2a}, and since, after irradiation, we have $m_{1a} << m_{2a}$, it follows that $n \approx m_{2a}$ during this time. Thus, Eq. (30) can be immediately integrated to find the concentration m_1 after t_D seconds of decay,

$$m_{1b} = m_{1a} \exp\left(-\frac{A_{m1} m_{2a}}{A_n N} \gamma t_D \right), \tag{31}$$

where the subscript b is used to indicate a value at the end of decay.

To find the decay of m_2, let us combine the low dose approximation, Eq. (19) with Eq. (27) to find

$$\frac{dm_2}{dt} = -\frac{A_{m2} m_2}{A_n N} n\gamma. \tag{32}$$

Since charge conservation requires $n = m_1 + m_2$, and since we have found that $m_1 << m_2$ is true for all of decay, we have $n \approx m_2$ and Eq. (32) can be immediately integrated to find m_2 after t_D seconds of decay,

$$n_b = m_{2b} = \frac{m_{2a}}{1 + \frac{A_{m2} m_{2a}}{A_n N} \gamma t_D}. \tag{33}$$

In sum, Eq. (31) shows that m_{1b} declines exponentially during decay while Eq. (33) shows that m_2 decays more slowly, because $A_{m1} >> A_{m2}$, and at a power rate, not an exponential rate.

3.3. Heating

A theory to explain the anomalous glow curve during heating and the kinetics that causes it will be developed. We start with some general equations, solutions of which are valid over the whole heating process. We then present simpler theories to explain the peak shape and magnitude for the first peak and then for the second peak. It will be shown that, as heating starts, there is an initial drop in m_1 as it recombines with electrons thermally freed from n. This is responsible for the first peak. Later in the heating process, m_1 is replenished from holes thermally released from m_2 and this enables more recombinations between free electrons and holes newly added to m_1. This process is responsible for the second peak.

3.4. Governing equations for heating

During heating with our chosen parameters, first γ and then γ_{m2} become important. Keeping both the γ and γ_{m2} terms but setting $X = 0$, the governing equations for m_1 and m_2, Eqs. (13) and (14), reduce to

$$\frac{dm_1}{dt} = \frac{B_1 M_1}{B_1 M_1 + B_2 M_2} m_2 \gamma_{m2} - \frac{A_{m1} m_1}{A_n (N - n) + A_{m2} m_2 + A_{m1} m_1} n\gamma, \tag{34}$$

$$\frac{dm_2}{dt} = \frac{B_1 M_1}{B_1 M_1 + B_2 M_2} m_2 \gamma_{m2} - \frac{A_{m2} m_2}{A_n (N - n) + A_{m2} m_2 + A_{m1} m_1} n\gamma. \tag{35}$$

From charge conservation, we know that $n = m_1 + m_2$. Also applying the low dose assumption as given by Eq. (19), Eq. (35) reduces to

$$\frac{dm_2}{dt} = -\frac{B_1 M_1}{B_1 M_1 + B_2 M_2} m_2 \gamma_{m2} - \frac{A_{m2}}{N A_n} \gamma (m_1 + m_2) m_2. \tag{36}$$

At the end of radiation and decay, and thus at the beginning of heating, we found that $m_1 << m_2$. Let us consider the case where m_1 is small enough that either

$$m_1 \ll m_2, \tag{37}$$

or

$$m_1 \ll \frac{\frac{B_1 M_1}{B_1 M_1 + B_2 M_2} \gamma_{m2}}{\frac{A_{m2}}{A_n N} \gamma}. \tag{38}$$

For the conditions of the numerical solution, one or the other of these two inequalities, Eq. (37) or Eq. (38) will be valid over the whole range of interest. Assuming that either Eq. (37) or Eq. (38), is valid, then Eq. (35) reduces to

$$\frac{dm_2}{dt} = -\frac{B_1 M_1}{B_1 M_1 + B_2 M_2} m_2 \gamma_{m2} - \frac{A_{m2}}{A_n N} \gamma {m_2}^2. \tag{39}$$

With the initial condition for m_2 provided by m_{2b} in Eq. (33), we can integrate Eq. (39) (see Appendix A) to find

$$m_2 = m_{2b} \frac{f(T)}{1 + \frac{A_{m2} m_{2b}}{A_n N} \int_{T_0}^{T} \gamma(T') f(T') dT' / \beta}, \tag{40}$$

where a linear temperature profile with heating rate β (K/s) has been assumed and where f is an abbreviation for

$$f(T) = \exp\left(-\frac{B_1 M_1}{B_1 M_1 + B_2 M_2} \int_{T_0}^{T} \gamma_{m2}(T') dT' / \beta \right). \tag{41}$$

Performing the integral yields

$$f(T) = \exp\left(-\frac{B_1 M_1}{B_1 M_1 + B_2 M_2} \frac{E_{m2} s_{m2}}{k\beta} [\Gamma(-1, E_{m2}/kT) - \Gamma(-1, E_{m2}/kT_0)] \right), \tag{42}$$

where Γ is the incomplete Gamma function

$$\Gamma(a, x) = \int_x^{\infty} e^{-x} z^{a-1} dz. \tag{43}$$

As usual, if the trap n is thermally stable at T_0, then the term $\Gamma(-1, E/kT_0)$ quickly becomes negligible as temperature increases.

To understand the meaning of $f(T)$, consider Eq. (36) under a hypothetical case in which $\gamma = 0$. In this case, m_2 decays like the usual first-order trap and its population would be $m_{2b} f(T)$. Alternatively, under a hypothetical case in which $\gamma_{m2} = 0$, then $f(T) = 1$. In this case, the solution of Eq. (40) yields second-order behavior. The validity of Eq. (40) for the general case, $\gamma \neq 0$ *and* $\gamma_{m2} \neq 0$, can be verified by substitution of the solution, Eq. (40) into the differential equation (39).

Next, we consider m_1. Starting with the conservation equation for m_1, Eq. (34), applying the low dose assumption, Eq. (19), and using charge conservation, $n = m_1 + m_2$, we have,

$$\frac{dm_1}{dt} = \frac{B_1 M_1}{B_1 M_1 + B_2 M_2} m_2 \gamma_{m2} - \frac{A_{m1} m_2}{A_n N} \gamma m_1 - \frac{A_{m1}}{A_n N} \gamma {m_1}^2. \tag{44}$$

Since, as per Eq. (40), m_2 is a known function of time, Eq. (44) is a first-order differential equation in a single variable, m_1. It can be readily solved numerically.

From Eq. (40) and Eq. (44), center concentrations m_1 and m_2 are known. Knowing these two and using charge conservation, we also know the trap population

$$n = m_1 + m_2. \tag{45}$$

n_c and n_v can then be readily computed from Eqs. (10) and (11). For heating, $X = 0$, and after applying the low-dose assumption, Eq. (19), these simplify to

$$n_c = \frac{n\gamma}{A_n N}, \tag{46}$$

$$n_v = \frac{m_2 \gamma_{m2}}{B_1 M_1 + B_2 M_2}. \tag{47}$$

The intensity during heating can then be computed with Eq. (8). This provides a complete solution for heating.

The next two subsections will examine the first and second peaks in more detail.

3.4.1. First peak

We will analyze the first TL peak to find both its magnitude and shape. For our chosen parameters, n becomes thermally unstable during heating before m_2 does. This means that γ becomes significant before γ_{m2}. It is during this time that the first peak occurs. We will find that it

has a first-order shape with an energy matching that of the electron trap n but with a dose-dependent effective s value.

During heating, we have $X = 0$ and, for the first peak, we have γ_{m2} negligible. Consequently, the same governing equations, (25) through (30) apply here as for the decay state. A difference is that γ, as given in Eq. (6), was a constant during decay, but, because it depends on temperature, is a variable here during heating. Just as during decay, Eqs. (28) and (29) imply that a large drop in m_1 occurs before there is a small change in m_2 or n. Thus, during the first peak, we can assume that n is little changed from its initial value before heating. Combining these considerations together and using condition (19), the integral of Eq. (26) becomes

$$m_1 = n_b \exp\left[-s_{eff} \int_0^t \exp(-E/kT(t'))dt' \right], \tag{48}$$

where s_{eff} is defined by

$$s_{eff} = \frac{A_{m1} n_b}{A_n N} s, \tag{49}$$

where n_b is the concentration of the electrons in the trap at the end of decay, Eq. (33). From Eq. (8), the intensity is $I = A_{m1} m_1 n_c$ where m_1 is given in Eq. (48) and n_c is given by Eq. (46) with $n = n_b$. Combining these considerations together with Eq. (6) and Eq. (48), an expression for intensity becomes

$$I = s_{eff} n_b \exp\left[-\frac{E}{kT} - s_{eff} \int_0^t \exp(-E/kT(t'))dt' \right]. \tag{50}$$

If we assume a linear temperature profile, $T = T_0 + \beta t$, the expression for intensity becomes (Lawless and Lo, 2001; Flores-Llamas and Gutiérrez-Tapia, 2013)

$$I = s_{eff} n_b \exp\left\{ -\frac{E}{kT} - \frac{E s_{eff}}{k\beta} [\Gamma(-1, E/kT) - \Gamma(-1, E/kT_0)] \right\}, \tag{51}$$

where Γ is the incomplete Gamma function, Eq. (43), and as before, if the trap n is thermally stable at T_0, then the term Γ(-1, E/kT_0) is negligible in Eq. (51) at the higher temperatures, T, at which the first peak occurs.

Since we have $n \approx m_2 \approx n_b$ during peak 1, we know that the integrated intensity of peak 1 is much less than n. This does not necessarily mean that peak 1 is small compared to peak 2, though because, depending on parameters, the integrated intensity of peak 2 may also be less than n.

In sum, the first peak exhibits first-order kinetics characterized by the energy of the electron trap, E, and an effective s given by Eq. (49). Note that, through n_b, the effective s depends on both the initial dose and the decay time and temperature. The integrated intensity of the first peak is m_{1b}.

3.4.2. Second peak

The radiative center, m_1, is depleted during the first peak. The second peak occurs when m_2 becomes thermally unstable, meaning that γ_{m2} becomes significant. Consequently, holes are thermally excited into the valence band, a fraction of which are captured by radiative center m_1. When holes in the newly increased population in center m_1 recombine with electrons being thermally excited from trap n, radiative emission grows resulting in the second peak. In this section, we will develop equations specific to the second peak, in particular the behavior of m_1 and intensity.

During the second peak, Eq. (40) remains valid for the concentration of the second trap, m_2. We will develop an equation for m_1 valid for the rising portion of the second peak. We start with Eq. (13), using again condition (19) and setting $X = 0$ we find

$$\frac{dm_1}{dt} = \frac{B_1 M_1}{B_1 M_1 + B_2 M_2} \gamma_{m2} m_2 - \frac{A_{m1}}{A_n N} \gamma (m_2 + m_1) m_1. \tag{52}$$

At the conclusion of the first peak, m_1 is depleted and $m_1 << m_2$. For as long as this remains true, Eq. (52) simplifies to

$$\frac{dm_1}{dt} = \frac{B_1 M_1}{B_1 M_1 + B_2 M_2} \gamma_{m2} m_2 - \frac{A_{m1} m_2}{A_n N} \gamma m_1. \tag{53}$$

Equation (53) shows that holes enter m_1 through the valence band after they are thermally released from m_1 and then holes are removed from m_1 by recombination with free electrons thermally released from the electron trap. If the recombination rate is sufficiently high, then the lifetime of holes in m_1 is short and the population of m_1 will be quasi-steady. Under this condition, the two terms on the right-hand-side of Eq. (53) balance each other,

$$\frac{B_1 M_1}{B_1 M_1 + B_2 M_2} \gamma_{m2} m_2 \approx \frac{A_{m1} m_2}{A_n N} \gamma m_1. \tag{54}$$

The term on the right in Eq. (54) is the radiative recombination rate of free electrons into center m_1. This is the emission intensity. Equation (54) says that the intensity is approximately equal to the left-hand-side of Eq. (54) which is the rate at which holes are thermally freed from m_2 and captured by m_1. If we solve Eq. (54) for the hole concentration in the radiative center, m_1 we have

$$\overline{m_1} = \frac{A_n N}{A_{m1}} \frac{B_1 M_1}{B_1 M_1 + A_2 M_2} \frac{\gamma_{m2}}{\gamma}, \tag{55}$$

where $\overline{m_1}$ denotes the quasi-steady value of m_1. One of the assumptions used to derive Eq. (55) is that $m_1 << m_2$ which implies $m_2 \approx n$. Note that $\overline{m_1}$ is independent of m_2 or n. This is because it represents a balance between creation of m_1 by thermal excitation from m_2 and destruction of m_1 by recombination with free carriers. The creation of m_1, represented by the right-hand-side of Eq. (54) is proportional to m_2. The destruction of m_1, represented by the right-hand-side of Eq. (54) is proportional to $m_2 \cdot m_1$. Consequently, when we solve Eq. (54) to find m_1, the factor of m_2 cancels out.

To assess the accuracy of the quasi-steady approximation here, we will develop a first estimate of how small dm_1/dt is by differentiating $\overline{m_1}$ with respect to time using Eqs. (6) and (7) to find

$$\frac{d\overline{m_1}}{dt} = \beta \frac{E_{m2} - E}{kT^2} \overline{m_1} \tag{56}$$

As long as the quasi-steady approximation is valid, an improved approximation can be obtained by substituting Eq. (56) into Eq. (53) and solving for $\overline{m_1}$ to find

$$\overline{m_1} = \frac{B_1 M_1}{B_1 M_1 + A_2 M_2} \frac{\gamma_{m2} m_2}{\frac{A_{m1} m_2}{A_n N} \gamma + \frac{(E_{m2} - E)\beta}{kT^2}}. \tag{57}$$

Using Eq. (57), we can obtain a better estimate of intensity. Using Eq. (8) for intensity, Eq. (10) for free electron concentration, n_c, and Eq. (57) for m_1, and remembering $n \approx m_2$, we have

$$I = \left[\frac{\frac{A_{m1} m_2}{A_n N} \gamma}{\frac{A_{m1} m_2}{A_n N} \gamma + \frac{(E_{m2} - E)\beta}{kT^2}} \right] \cdot \left(\frac{B_1 M_1}{B_1 M_1 + A_2 M_2} \gamma_{m2} m_2 \right). \tag{58}$$

The quantity in square brackets in Eq. (58) is the correction to the quasi-steady approximation which, while the quasi-steady approximation is accurate, is just slightly less than one. The quantity in parentheses is the rate at which holes are released from m_2 into the valence band and subsequently captured by m_1. Thus, the intensity during this period is controlled by the rate at which holes are released from m_2. The concentration of m_2 is given by Eq. (40).

Among the assumptions used to derive Eq. (58) was that $m_1 << m_2$. To assess the validity of this assumption, let us look again at Eq. (55). The only terms on the right-hand-side of Eq. (55) that vary with temperature are the thermal excitation rates γ and γ_{m2}. For our chosen parameters we have

$$E_{m2} > E. \tag{59}$$

This means that γ_{m2}/γ will be small at low temperature but increase rapidly as temperature increases. Consequently, m_1 grows as temperature increases at the same time that m_2 is decreasing. This means that the $m_1 << m_2$ assumption will fail at a sufficiently high temperature during heating. For our chosen parameters, this happens after the second peak occurs.

In sum, under the assumptions made, the intensity of the second peak is given by Eq. (58). During this time, the populations of m_1 and m_2 are given by Eqs. (57) and (40), respectively.

3.4.3. Corrections for higher dose

In previous sections, the analysis assumed, for simplicity, low dose: $n << N$. Since the simulations were done with $n/N = 0.1$, one might expect that this assumption would cause an $O(10\%)$ error. We will develop here some first-order corrections for doses that are small but not very small. The formulas of the previous sections have the advantage of being simpler and therefore providing a clearer picture of dominant processes and how they interact. The formulas here are more complex but may be useful if one desires higher numerical accuracy.

The first set of corrections is for the decay stage. We again start with Eqs. 25–27. We will again assume $m_1 << m_2$ which, by charge conservation, implies that $m_2 = n$. We will also again assume $A_{m1}m_1 + A_{m2}m_2 << A_nN$ but, this time, we will not assume that n or m_2 is small compared to N. In this case, Eq. (27) reduces to

$$\frac{dm_2}{dt} = -\frac{A_{m2}m_2^2}{A_n(N-m_2)}\gamma. \tag{60}$$

Equation (60) can be immediately integrated to find

$$\frac{N}{m_{2a}} - \frac{N}{m_2} - \ln\left(\frac{m_2}{m_{2a}}\right) = \frac{A_{m2}}{A_n}\gamma t_D, \tag{61}$$

where m_{2a} is again the trap concentration at the start of decay. Equation (61) can be solved explicitly for m_2 as follows,

$$m_2 = \frac{-N}{W_{-1}\left[-\frac{N}{m_{2a}}\exp\left(-\frac{A_{m2}}{A_n}\gamma t_D - \frac{N}{m_{2a}}\right)\right]}, \tag{62}$$

where W_{-1} is the $k = -1$ branch of the Lambert W function.[1] To obtain an improved estimate for m_1, we integrate Eq. (28) to find

$$\frac{m_1}{m_{1a}} = \left(\frac{m_2}{m_{2a}}\right)^{A_{m1}/A_{m2}} \tag{63}$$

Combining Eq. (62) with Eq. (63), we have

$$m_1 = m_{1a}\left[\frac{-N/m_{2a}}{W_{-1}\left[-\frac{N}{m_{2a}}\exp\left(-\frac{A_{m2}}{A_n}\gamma t_D - \frac{N}{m_{2a}}\right)\right]}\right]^{A_{m1}/A_{m2}}. \tag{64}$$

Equations (63) and (64) agree well with the simulation as shown in Section 4.

We also need to develop a dose correction to m_2 for the heating stage. Starting with Eq. (35) and again assume $m_1 << m_2$ which, by charge conservation, implies that $m_2 \approx n$ and $A_{m1}m_1 + A_{m2}m_2 < A_nN$ but without assuming that m_2 is small, we find

$$\frac{dm_2}{dt} = \left(\frac{B_1M_1}{B_1M_1 + B_2M_2}\gamma_{m2}\right)m_2 - \left(\frac{A_{m2}}{A_n}\gamma\right)\frac{m_2^2}{N-m_2}. \tag{65}$$

We can expand $1/(N\text{-}m_2)$ in a Taylor series,

$$\frac{1}{N-m_2} = \frac{1}{N}\left[1 + \frac{m_2}{N} + \left(\frac{m_2}{N}\right)^2 + \ldots\right]. \tag{66}$$

Using this expansion, Eq. (65) becomes

$$\frac{dm_2}{dt} = \left(\frac{B_1M_1}{B_1M_1 + B_2M_2}\gamma_{m2}\right)m_2 - \left(\frac{A_{m2}}{A_nN}\gamma\right)m_2^2\left[1 + \frac{m_2}{N} + \left(\frac{m_2}{N}\right)^2 + \ldots\right]. \tag{67}$$

After much math (see Appendix B) and neglecting terms of order $(m_2/N)^2$ or smaller, we find

$$m_2 = m_{2,0} - \int_0^t \frac{A_{m2}m_{2,0}(t')^3}{N^2}\gamma(t')\exp\left(-\int_0^{t'}\left[2\frac{A_{m2}m_{2,0}(t'')}{A_nN}\gamma(t'') + \frac{B_1M_1}{B_1M_1 + B_2M_2}\gamma_{m2}(t'')\right]dt''\right)dt', \tag{68}$$

where t' and t'' are integration variables and $m_{2,0}$ refers to the low-dose solution of Eq. (40).

As discussed in Section 5, the analytical theory and the numerical simulation are in excellent agreement.

3.5. Numerical-simulation results

To demonstrate anomalous fading, we have chosen a set of plausible parameters and solved numerically the set of simultaneous differential equations (1)–(5) by using the Matlab solver ode23tb designed to solve stiff differential equations. The set of parameters chosen was (see Fig. 1): $N = 10^{16}\text{cm}^{-3}$; $A_n = 10^{-5}\text{cm}^3\text{s}^{-1}$; $E = 0.385\text{eV}$; $s = 10^7\text{s}^{-1}$; $M_1 = 10^{17}\text{cm}^{-3}$; $A_{m1} = 2 \times 10^{-8}\text{cm}^3\text{s}^{-1}$; $B_1 = 10^{-7}\text{cm}^3\text{s}^{-1}$; $M_2 = 10^{17}\text{cm}^{-3}$; $A_{m2} = 10^{-9}\text{cm}^3\text{s}^{-1}$; $B_2 = 10^{-5}\text{cm}^3\text{s}^{-1}$; $E_{m2} = 1.34\text{eV}$; $s_{m2} = 5 \times 10^{12}\text{s}^{-1}$.

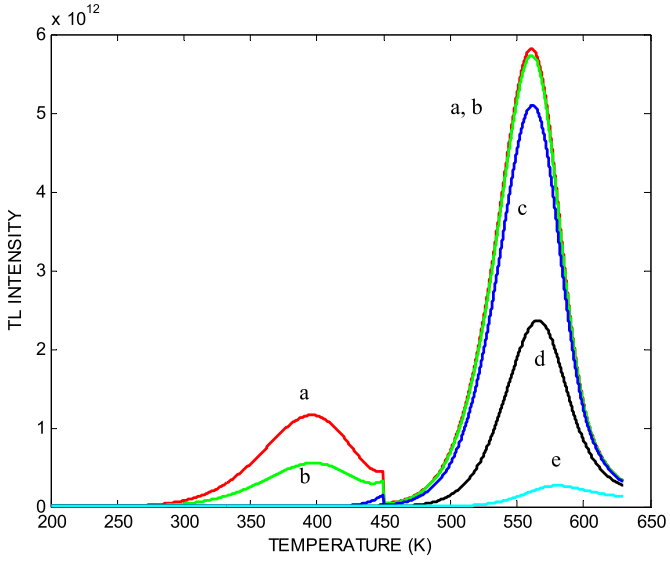

Fig. 2. Simulated glow curves showing the anomalous fading effect. The simulated excitation was performed at 100K, the sample was then held for different periods of time at 300K and then the heating was simulated from 200K up. Intensities below 450K are multiplied by 10. Holding times at 300K are: (a) 1s; (b) 10^3s; (c) 10^4s; (d) 10^5s; (e) 10^6s.

[1] To verify that the special function library is returning the desired branch, calculate $W_{-1}(-4\exp(-4))$. The correct result is -4.

The rate of production of electron-hole pairs during irradiation was chosen as $X = 5 \times 10^7 \text{cm}^{-3}\text{s}^{-1}$ and the time of excitation $t_D = 2 \times 10^7$s, so that the total concentration of electron-hole pairs produced (to which the total dose is proportional) is $D = 10^{15}\text{cm}^{-3}$.

The simulated excitation was performed at 100K, the sample was then held for different periods of time at 300K and then the heating was simulated from 200K up. The results of the simulations are shown in Fig. 2. Note that the intensities below 450K have been multiplied by 10 so that the behavior in this range can be seen. Curve (a) (red line) shows the results right after excitation, with fading time of 1 s. Curve b (green) shows the results following 10^3s fading time. The first peak has decayed to about half of the intensity whereas the second peak had only minimal decay. Curve c (blue) following 10^4s fading time shows that the first peak has practically vanished, and the second peak has lost ~12% of the intensity. In curve d (black) following 10^5 s decay the second peak is ~40% of the original intensity. In curve e (cyan), following 10^6s the decay is down to ~5% of the initial intensity right after excitation. It is worth mentioning that the high-temperature peak shifts to higher temperature as it fades, from ~560K to ~580K. Also, the peak shape changes gradually from having a nearly first-order appearance with short fading time to more like second-order shape following a longer decay time.

Fig. 3 shows the dependence of the maximum TL intensity of the two peaks on fading time. Note that the time scale is logarithmic varying from 1s to 10^6s. The higher-temperature peak is seen to reduce to ~5% of its initial value in 10^6s whereas the low-temperature peak is practically nil after 10^4s.

Fig. 4, based on the equations of subsection 3.3.1, shows the same two peaks, at ~400K and ~560K as determined by the approximate theory. The fading times are the same as in Fig. 2. Like in the presentation of the numerical solution of the differential equations, following this decay time, the first peak practically disappears after decay time of 10^4s and the intensity of the second peak reduces to ~40% of the initial intensity. The close similarity between the curves in Figs. 2 and 4 which includes the temperatures of occurrence of the two peaks and their relative intensity, attests to the correctness of the two approaches. The difference between the intensities in Figs. 2 and 4 is seen to be less than 4%.

Fig. 5 shows the decay of the occupancies with holding time up to 10^5 s at 300K. Since m_1 is much smaller than m_2, n and m_1 behave in practically the same way during this time span, decaying rather

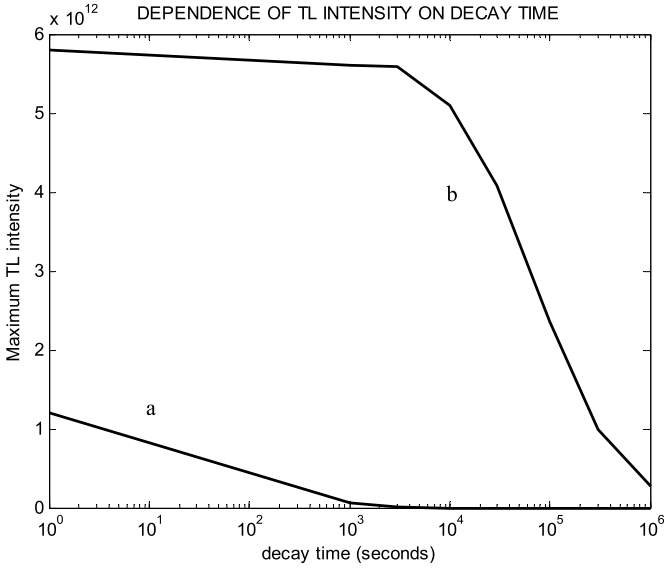

Fig. 3. Dependence of the maximum simulated TL intensities on the fading time. (a) is for the low-temperature peak and (b) for the higher temperature peak. Holding temperature was 300K.

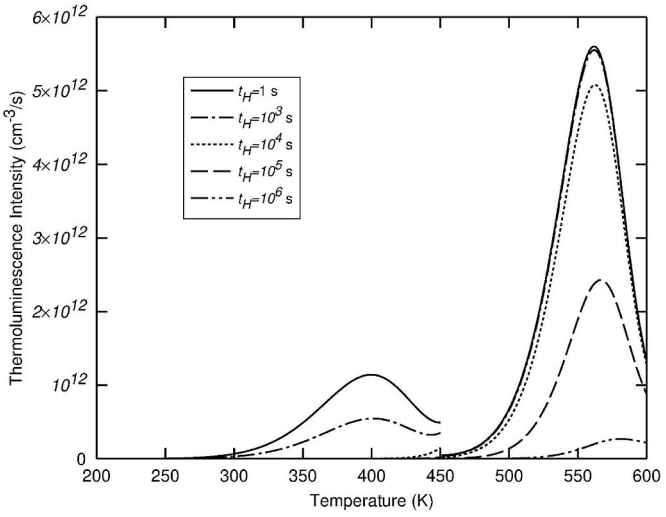

Fig. 4. The glow peaks determined by the theory, Eq. (51) (first peak) and Eq. (58) (second peak) following the same decay times as in Fig. 2. Here, t_H indicates holding time.

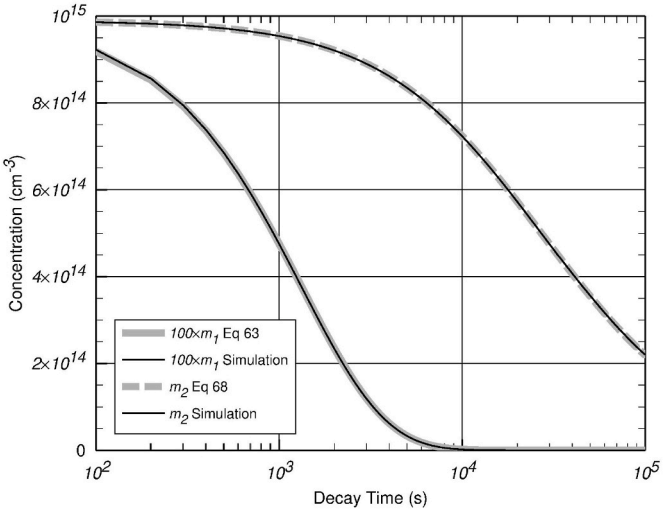

Fig. 5. The dependence of the traps and center occupancies after excitation as a function of holding time at 300K, as determined by the numerical solution of Eqs. (1)–(5), following the simulated excitation, and by the analytical approach, on a semi-logarithmic scale. The concentrations n and m_2 are nearly the same since m_1, n_c and m_v are relatively small. The solid black lines represent the simulation and the grey lines show the results of the theory.

significantly. The values of m_1 have been multiplied by 100 so that the fast decaying curve can be seen on the same graph. It is shown that practically the same results were reached by the numerical simulation and by the theoretical approach with approximations.

3.6. Analysis of the results

We would like to consider the analysis of the numerical results. It is quite obvious that the TL peaks we see may not be of first or second-order and, for that matter, neither have exactly the shape of a general-order peak. However, we do have a TL peak which has a conventional shape, which may be close to being symmetric similarly to a second-order peak or be asymmetric, looking like a first-order peak, or anything in between. Not having better tools in hand, we have used the available ones to get the *effective* activation energy, frequency factor and order of kinetics.

A simple home-made curve-fitting program has been used to evaluate the three mentioned effective parameters of the second peak (see e.g. Shenker and Chen (1971)). We have simulated a glow curve with a heating rate $\beta_1 = 1$K/s. The curve-fitting yielded the following effective parameters for the peak at 561K: $E_{eff} = 1.25$eV; $\mu_g = 0.445$; $s_{eff} = 8.5 \times 10^9 s^{-1}$. It should be mentioned that although in this case, the shape factor μ_g is in the range between that of first- and second-order (0.42–0.52), it is much closer to being of first order. The activation energy and frequency factor may be compared to the values of $E_{m2} = 1.34$eV; $s_{m2} = 5 \times 10^{12} s^{-1}$. The differences between the evaluated E and s and the inserted ones should not be surprising; the complex situation of transitions of both electrons and holes influences the results, which is reflected in the magnitude of the effective parameters.

Another way of analyzing a glow peak is by using the different heating rates method. We then simulated the glow curve with $\beta_2 = 2$K/s and the second peak occurred at 575.4K. We have then used the well known equation for evaluating the activation energy from two heating rates measurement (see e.g., Booth (1954)),

$$E_\beta = k \frac{T_1 T_2}{T_1 - T_2} \ln \left[\frac{\beta_1}{\beta_2} \left(\frac{T_2}{T_1} \right)^2 \right]. \quad (69)$$

Substituting the two maxima temperatures T_1, T_2 and the two heating rates (1 and 2K/s), this yielded $E_\beta = 1.24$eV, with rather surprising agreement with the value reached by the peak-shape method and not too far from the inserted value of $E_{m2} = 1.34$eV.

It was also interesting to analyze the low temperature peak by the same curve fitting method. For the same excitation of $X = 5 \times 10^7 cm^{-3}s^{-1}$ and $t_D = 2 \times 10^7$s, we found $E_{\text{eff}} = 0.42$eV, with reasonably good agreement with the inserted value of $E = 0.385$eV. The effective frequency factor was found to be $s_{eff} = 8 \times 10^3 s^{-1}$, about three orders of magnitude smaller than the inserted one. Here, however, we have to consider Eq. (49) which shows that s_{eff} depends on s, A_n, A_{m1}, N, and n_b. Since the latter depends on the dose, it is obvious that s_{eff} may get different values, depending on the dose. The symmetry factor has been found to be $\mu_g = 0.465$, intermediate between the symmetry of first and second order peaks. Due to the rather complex process taking place here, this value which indicates an effective order of kinetics of ~1.5, should not be considered strange.

Another feature of the simulated peaks that was tested was the dose dependence. The results are shown in Fig. 6. With a constant time of excitation of $t_D = 2 \times 10^7$s and different dose rates X varying from $2.5 \times 10^6 cm^{-3}s^{-1}$ in curve (a) and multiplied by factors of 2 in successive curves (b-e). At the low dose, the peak shape looks approximately as a second-order peak and it also shifts to lower temperature with increasing dose, again, typical of second-order kinetics. At higher doses, the shape as seen by the symmetry of the peak has first-order features, and there is no further temperature shift of the maximum. As for the dose dependence, it starts being nearly linear at low doses and becomes sublinear at higher doses. It seems that this does not represent real approach to saturation. In the highest-dose peak shown, the initial concentration of electrons before heating was recorded and it was $n_0 = 1.6 \times 10^{15}$ cm^{-3}, which is only 16% of the trap concentration, $N = 10^{16} cm^{-3}$. m_{20} is nearly the same as n_0 and $m_{10} \sim 10^{13} cm^{-3}$. M_1 and M_2 are $10^{17} cm^{-3}$ and therefore their relative initial occupancy before heating is significantly lower. The sublinearity should therefore be ascribed to dynamic equilibrium rather than real saturation.

We have also looked for a possible dose-rate effect. For one of the doses, we increased the dose-rate by a factor of 10 and decreased the time of excitation by the same factor of 10. The results came out identical, meaning that no dose-rate effect occurred, as suggested in section 3.1 above.

Finally, Fig. 7 has a similar appearance to Fig. 6, but depicts a different feature, namely, the fading-temperature dependence of the simulated TL curve. The excitation is the same in all the cases shown, namely, excitation is at a rate of $X = 5 \times 10^7 cm^{-3}s^{-1}$ and for a time $t_D = 2 \times 10^7$s. The time of fading is 10^5s in all the curves and the excitation temperature is 100K. The fading temperatures were (a) 290K; (b) 300K; (c) 310K; (d) 320K; (e) 330K; (f) 340K; the strong dependence on the fading-temperature is clearly seen.

4. Discussion

In the present work, we propose an energy level model consisting of an electron trap, a hole trap and a hole luminescence center to explain the anomalous-fading effect occurring quite often in thermoluminescence (TL) materials. We assume that in the range of occurrence of the glow curve, electrons can be released from an electron trap into the conduction band and holes from a hole trap into the valence band. As mentioned above, the present model resembles to some extent to that previously suggested by Schön and Klasens. However, their model

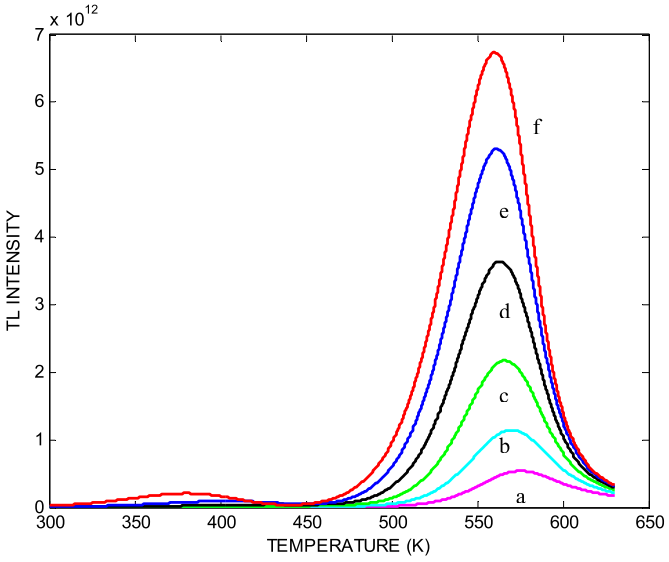

Fig. 6. Dose dependence of the simulated glow curve. The simulated time of excitation was 2×10^7s and the excitation dose rates (X) were: (a) $2.5 \times 10^6 cm^{-3}s^{-1}$; (b) $5 \times 10^6 cm^{-3}s^{-1}$; (c) $1 \times 10^7 cm^{-3}s^{-1}$; (d) $2 \times 10^7 cm^{-3}s^{-1}$; (e) $4 \times 10^7 cm^{-3}s^{-1}$; (f) $8 \times 10^7 cm^{-3}s^{-1}$.

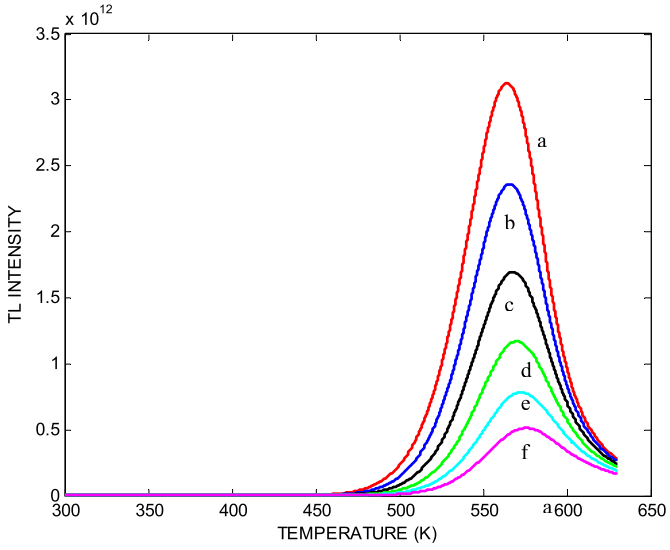

Fig. 7. Dependence of the simulated glow curves on the temperature of fading. The temperatures were: (a) 290K; (b) 300K; (c) 310K; (d) 320K; (e) 330K; (f) 340K.

includes only two energy levels (see also McKeever, 1985, P. 61) and the present model has the three participating energy levels seen in Fig. 1. The transitions of the two kinds of charge carriers during the different steps of the simulated experiment are seen to produce the anomalous effect. The results of the simulations show directly the anomalous fading effect of the high-temperature peak. When the simulated sample is held close to room temperature, at 300K, the second peak in the range of 560–580K (around 300 °C) decays to ~1/e of its original intensity in $\sim 10^5$s, or ~28 h. As can be seen in Fig. 2, the shape of the peak varies with fading times, and therefore, analysis based on the shape of the peak does not yield a unique expected decay time. However, the effective values we found by the analysis were between 10^{11} and 10^{15}s, many orders of magnitude higher than the decay times of $\sim 10^5$s found in the simulations, hence the anomalous behavior. Obviously, even without relating to these numbers, it is evident that decay to ~1/e of a peak occurring at ~300 °C when the sample is held at RT for 28 h is anomalous. It should be noted that the results of the numerical simulations are reached without any simplifying assumptions or approximations. Putting it in a different way, a peak with apparent activation energy of 1.24eV fading significantly at 300K definitely means anomalous fading.

As for the analytical approach with approximations, from Eq. (33) we know that the fading of m_{2b} is controlled by the E and s of the electron trap. Because E is small, m_{2b} is fading at low temperature. m_{2b} appears twice in Eq. (40), and when it decays, obviously the TL intensity decays as well. From Eq. (40) we see that the glow curve is delayed until the second trap, characterized by E_{m2}, s_{m2}, becomes thermally unstable. Because E_{m2} is large, the glow peak occurs at high temperature. In sum, fading is controlled by E and s while the peak temperature is strongly influenced by E_{m2} and s_2. Thus, under this energy-level model, the fading and the peak temperature are partly decoupled from each other. Note that the present model explains the temperature-dependent fading which, as described above, occurs in some materials. Examples of temperature-dependent anomalous fading have been given by Wintle (1977). The dependence of the glow curves on the temperature of fading as shown in Fig. 7 is as expected from the model and in qualitative agreement with the temperature-dependent experimental results appearing in the literature and mentioned in the introduction.

As pointed out above, using the two approaches of numerical solution of the differential equations and the theoretical approach with approximations yielded very similar glow curves. This includes the occurrence of the two peaks at ~400K and ~560K, their relative intensities and the fading behavior with time. Note that with the higher-dose correction, there is a difference of less than 4% in the simulated intensity between the two approaches as seen in curve (a) in Fig. 2 and the solid line in Fig. 4. This small difference can be attributed to the approximations in the theoretical approach and perhaps to some inaccuracy in the numerical solution as well. Thus, the curves as shown on Figs. 2 and 4 are practically the same with the two peaks occurring at the same temperatures, and with the same relative intensities and the same shapes.

To get a better insight into the process that takes place during the heating, following fading time, we have plotted the occupancies m_1. m_2, n_c, n_v and the intensity I in Fig. 8 as functions of temperature. Note that n is not shown since along most of the range it nearly coincides with m_2. The occurrence of the TL peak in this system is associated with the peak shape of m_1 and n_c. The TL peak is proportional to the product $m_1 \times n_c$ (see Eq. (8)). As seen in these two figures, m_1 has a peak at ~575K and n_c at ~528K. The resulting TL peak which is their product appears in between, at ~560K. An important fact to note here is that the values of n, m_1 and m_2 are more than six orders of magnitude larger than n_c, a point that we used in the approximations.

It is clear that the evaluated activation energy of ~1.25eV is closer to the inserted hole activation energy than to that of the electrons which seems to show that although the process is of electrons being released and recombining with holes in centers, the limiting factor is the availability of holes coming from the hole trap, and recombining after a short

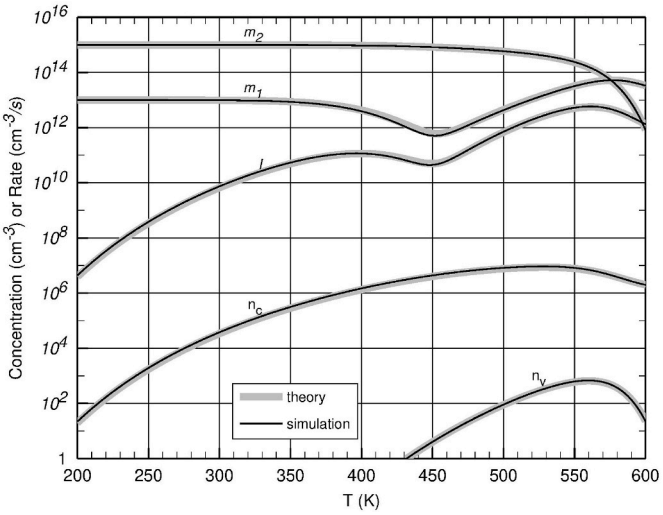

Fig. 8. With the same parameters, the temperature dependence of the occupancies m_1, m_2, n_c and n_v along with the TL intensity I as determined by the numerical solution of the differential equations and the analytical approximation approach are shown during the heating stage on a semi-log scale. The solid black lines represent the results of the simulation and the grey lines show the results of the theory.

stay in M_1. In more detail, immediately after the first peak subsides, the electrons released from the trap N recombine primarily with holes in M_2 releasing, as we assumed, no radiation. The trap population, n, continues its radiationless decline until m_2 becomes thermally unstable. Because $A_{m1} >> A_{m2}$, holes in M_1 stay only a short time before they recombine with electrons in N, releasing radiation. This creates the second peak. The "recombination after short stay in m_1" is the basis for the quasi-steady assumption for m_1 during the second peak, expressed as Eq. (54) above.

As pointed out above, the present energy-level model of anomalous fading is the same as that previously published by Lawless et al. (2021) on the inability to excite in some cases a relatively high-temperature peak at a certain range of temperatures of excitation. The ranges of the chosen sets of trapping parameters used to demonstrate the two effects have been quite different. It is not surprising, however, that the two effects can be explained by the same model since the effects described are closely related. In the former, the higher temperature peak from a set of two peaks diminishes very quickly at rather low temperatures and in the latter, the second peak of the two cannot be excited to begin with.

5. Conclusions

The present model is a possible alternative to the mentioned model of tunneling. There is no claim here that there is something wrong with the tunneling model for explaining anomalous fading; we only suggest the present model as a viable alternative. Since tunneling is a localized transition and the present model deals with delocalized transitions, we suggest that in an experiment, two contacts are applied to the sample and the thermally stimulated conductivity (TSC) will be measured. If no TSC is measurable, probably it is tunneling whereas the occurrence of a TSC peak would indicate the present model.

In conclusion, the results of this model gave a normal-looking TL peak which yielded reasonable effective parameters and rather normal dose dependence and lack of dose-rate dependence. The main new feature of the model is the occurrence of anomalous fading effect whereby, a peak occurring at ~300 °C (573K) and having an apparent activation energy of ~1.25 eV decays quite significantly when the sample is held at room temperature within 24 h in the given example.

Declaration of competing interest

The authors declare that they have no known competing financial interests or personal relationships that could have appeared to influence the work reported in this paper.

Data availability

Data will be made available on request.

Appendix A. Derivation of Eq. (40)

Let us define abbreviations a and b,

$$a = \frac{A_{m2}}{A_n N}\gamma \quad and \quad b = \frac{B_1 M_1}{B_1 M_1 + B_2 M_2'}\gamma_{m2}. \tag{A1}$$

With these definitions, Eq. (36) can be written as

$$\frac{dm_2}{dt} = -am_2{}^2 - bm_2, \tag{A2}$$

where $a = a(t)$ and $b = b(t)$ are functions of time. Equation (A2) is a nonlinear first-order differential equation with variable coefficients. To solve it, the first step is to convert it to a linear differential equation. To do this, we first define a new variable $f = f(t)$ by

$$f = \exp\left(-\int_0^t b(t')dt'\right), \tag{A3}$$

where t' is a variable of integration. It follows that

$$b = -\frac{1}{f}\frac{df}{dt}. \tag{A4}$$

Substituting Eq. (A4) into Eq. (A2) and rearranging to place the derivatives on one side, one gets

$$\frac{m_2}{f}\frac{df}{dt} - \frac{dm_2}{dt} = am_2{}^2. \tag{A5}$$

Multiplying both sides of Eq. (A5) by f/m_2^2, we have

$$\frac{1}{m_2}\frac{df}{dt} - \frac{f}{m_2{}^2}\frac{dm_2}{dt} = af. \tag{A6}$$

Equation (A6) can be simplified to

$$\frac{d(f/m_2)}{dt} = af. \tag{A7}$$

If we define a new variable $y = f/m_2$, we can see that Eq. (A7) becomes a linear differential equation,

$$\frac{dy}{dt} = af. \tag{A8}$$

Equation (A8) can be immediately integrated to find

$$y(t) - y(0) = \int_0^t a(t')f(t')dt', \tag{A9}$$

where t' is again a variable of integration. If we replace y with its definition, f/m_2, Eq. (A9) becomes

$$\frac{f}{m_2} - \frac{1}{m_{2b}} = \int_0^t a(t')f(t')dt', \tag{A10}$$

where we have used the fact that, from Eq. (A3), the value of f at $t = 0$ is $f(0) = 1$. Finally, solving Eq. (A10) for m_2, we find

$$m_2 = \frac{m_{2,0}f}{1 + m_{2,0}\int_0^t a(t')f(t')dt'}. \tag{A11}$$

If we convert the independent variable from time t to temperature T and use the definition of a from Eq. (A1), then Eq. (A11) becomes Eq. (40) in the main text. Similarly, substituting the definition of b from Eq. (A1) and changing independent variable, Eq. (A3) becomes Eq. (41).

Appendix B. Perturbation Expansion

First, let us note that Eq. (67) has the form

$$\frac{dm_2}{dt} = -bm_2 - am_2{}^2\left[1 + \varepsilon\frac{m_2}{m_{2b}} + \varepsilon^2\left(\frac{m_2}{m_{2b}}\right)^2 + \ldots\right], \tag{B1}$$

where $a = a(t)$ and $b = b(t)$ are known functions of time, m_{2b} is the concentration of m_2 at the start of heating, and where we have defined

$$\varepsilon = \frac{m_{2b}}{N}. \tag{B2}$$

ε is the fraction of trap N that is occupied after the end of decay. Note that, during heating, $m_2 \leq m_{2b}$ and thus the second term in the square brackets in Eq. (B1), $\varepsilon m_2/m_{2b}$, is, during heating, no longer larger than ε. We will treat ε as a small parameter and obtain the first order to m_2 for ε being small but non-zero. According to Eq. (B2), m_2 will be a function of time and of ε,

$$m_2 = m_2(t, \varepsilon). \tag{B3}$$

m_2 is subject to the initial condition

$$m_2(0, \varepsilon) = m_{2b}. \tag{B4}$$

We expand Eq. (B3) into a power series in ε,

$$m_2 = m_{2,0}(t) + \varepsilon m_{2,1}(t) + \varepsilon^2 m_{2,2}(t) + \ldots \tag{B5}$$

where $m_{2,0}$, $m_{2,1}$, $m_{2,2}$ and so on are as-yet-undetermined functions of time. This approach is called a *perturbation expansion*. Perturbation expansions are used in many fields of physics including quantum mechanics, see Chap. 16 of Messiah (1963) or Chap. 17 of Merzbacher (1970) and fluid mechanics, Sears (1960). See also Part 3 of Bender and Orszag (1978). It is important to note that $m_{2,0}$, $m_{2,1}$, $m_{2,2}$ …, are not functions of ε. Substituting Eq. (B5) into Eq. (B1), we find

$$\frac{dm_{2,0}}{dt} + \varepsilon \frac{dm_{2,1}}{dt} + \varepsilon^2 \frac{dm_{2,2}}{dt} + \ldots = -b\left[m_{2,0}(t) + \varepsilon m_{2,1}(t) + \varepsilon^2 m_{2,2}(t) + \ldots\right]$$

$$-a\left[m_{2,0}(t) + \varepsilon m_{2,1}(t) + \varepsilon^2 m_{2,2}(t) + \ldots\right]^2 \left[1 + \varepsilon\left(\frac{m_2(t)}{m_{2b}}\right) + \varepsilon^2\left(\frac{m_2(t)}{m_{2b}}\right)^2 + \ldots\right]. \tag{B6}$$

After collecting together terms with the same powers of ε, Eq. (B6) becomes

$$\left[\frac{dm_{2,0}}{dt} + a{m_{2,0}}^2 + b m_{2,0}\right] + \varepsilon\left[\frac{dm_{2,1}}{dt} + 2a m_{2,0} m_{2,1} + a{m_{2,0}}^3 / b m_{2,1}\right] + O(\varepsilon^2) = 0. \tag{B7}$$

Note that, by assumption, nothing inside the square brackets depends on ε. For Eq. (B7) to remain true for varying values of ε, it must be that each quantity in square brackets is zero separately.[2] Taking the first square brackets in Eq. (B7) and setting it to zero, we have

$$\frac{dn_0}{dt} = -a{m_{20}}^2 - b m_{20}. \tag{B8}$$

Taking the second square bracket and setting it to zero we get

$$\frac{dm_{2,1}}{dt} + (2a m_{2,0} + b) m_{2,1} = -a{m_{2,0}}^3 / m_{2b}. \tag{B9}$$

For each differential equation (B8) and (B9), we need initial conditions. Substituting Eq. (B5) into Eq. (B4), we have

$$m_{2b} = m_{2,0}(0) + \varepsilon m_{2,1}(0) + \varepsilon^2 m_{2,2}(0) + \ldots . \tag{B10}$$

Again, collecting terms with the same power of ε,

$$0 = \left[m_{2,0}(0) - m_{2b}\right] + \varepsilon\left[m_{2,1}(0)\right] + \varepsilon^2\left[m_{2,2}(0)\right] + \ldots . \tag{B11}$$

Again, no term inside the square brackets depends on ε. If Eq. (B11) is to be valid even as ε varies, it follows that each square bracket must be zero separately. Taking just the first two brackets one gets

$$m_{2,0}(0) = m_{2b}, \tag{B12}$$

$$m_{2,1}(0) = 0. \tag{B13}$$

The first step is to solve Eq. (B8) subject to initial condition Eq. (B12). The solution is given by Eq. (A10),

$$m_{2,0} = m_{2,b} \frac{f(t)}{1 + \int_0^t a(t') f(t') dt'} \tag{B14}$$

The next step is to solve Eq. (B9) subject to initial condition (B13). Equation (B9) is a linear first-order differential equation with variable coefficients. By standard methods, (Ince, 1956), its solution is

$$m_{2,1} = -\int_0^t \frac{a(t') m_{2,0}(t')^3}{m_{2b}} \exp\left(-\int_0^{t'} \left[2a(t'') m_{2,0}(t'') + b(t'')\right] dt''\right) dt'. \tag{B15}$$

Equation (B15) provides the first-order-in-ε correction to m_2 for non-zero dose. We will neglect higher order corrections. To obtain our final

[2] Equation (B7) is a polynomial in variable ε. It is a theorem of linear algebra that, if a polynomial of a continuous variable is zero everywhere, then each of its coefficients must be zero.

estimate for m_2 during heating, we substitute solutions Eq. (*B*14) and Eq. (*B*15) into Eq. (*B*5) and use the definitions in Eq. (*B*2) and (*A*1). The result is expressed in Eq. (68).

References

Bender, C.M., Orszag, S.A., 1978. Advanced Mathematical Methods for Scientists and Engineers. McGraw-Hill, New York.

Bringuier, E., 2020. Disorder-enhanced luminescence kinetics in volcanic feldspars. EPJ Web of Conferences, EDP Sciences 2020 (244), 1–6.

Booth, A.H., 1954. Calculation of electron trap depths from TL maxima. Can. J. Phys. 32, 214–215.

Bowman, S.G.E., 1988. Observations of anomalous fading in maiolica. Nucl. Tracks Radiat. Meas. 14, 131–137.

Bull, C., Garlick, G.F.J., 1950. The luminescence of diamonds. Proc. Phys. Soc., London 63, 1283–1291.

Chen, R., Hag-Yahya, A., 1997. A new possible interpretation of the anomalous fading in thermoluminescent materials as normal fading in disguise. Radiat. Meas. 27, 205–210.

Chen, R., Pagonis, V., Lawless, J.L., 2008. Duplicitous thermoluminescence peak associated with a thermal release of electrons and holes from trapping states. Radiat. Meas. 43, 162–166.

Devi, M., Chauhan, N., Rajapara, H., Joshi, S., Singhvi, A.K., 2022. Multispectral athermal fading rate measurements in K-feldspar. Radiat. Meas. 156, 106804.

Flores-Llamas, H., Gutiérrez-Tapia, C., 2013. Thermoluminescence glow curve deconvolution functions for continued fractions by different orders of kinetics. Radiat. Eff. Defect Solid 168, 163–175.

Garlick, G.F.J., Robinson, I., 1972. The thermoluminescence of lunar samples. Symp. - Int. Astron. Union 47, 324–329.

Guérin, G., Visocekas, R., 2015. Volcanic feldspars anomalous fading: evidence for two different mechanisms. Radiat. Meas. 79, 1–6.

Hoogenstraaten, W., 1958. Electron traps in ZnS phosphors. Philips Res. Rep. 13, 515–693.

Ince, E.L., 1956. Ordinary Differential Equations. Dover, New York.

Jaek, I., Molodkov, A., Vasilchenko, V., 2007. Possible reasons for anomalous fading in alkali feldspars used for luminescence dating of Quaternary deposits. Est. J. Earth Sci. 56, 167–178.

Kieffer, F., Meyer, F., Rigaut, J., 1971. Is isothermal deferred luminescence in organic glasses due to electron tunnelling? Chem. Phys. Lett. 11, 359–361.

Kitis, G., Polymeris, G.S., Pagonis, V., Tsirliganis, N.C., 2006. Thermoluminescence response and apparent anomalous fading factor of Durango fluorapatite as a function of the heating rate. Phys. Status Solidi 203, 3816–3823.

Klasens, H.A., 1946. Transfer of energy between centres in zinc sulphide phosphors. Nature (London) 158, 306–307.

Kumar, R., Kook, M., Jain, M., 2022. Does hole instability cause anomalous fading of luminescence in feldspar? J. Lumin. 252, 119403.

Lawless, J., Lo, D., 2001. Thermoluminescence for nonlinear heating profiles with application to laser heated emissions. J. Appl. Phys. 89, 6145–6152.

Lawless, J.L., Chen, R., Pagonis, V., 2021. A model explaining the inability of exciting thermoluminescence (TL) peaks in certain low temperature ranges. Radiat. Meas. 145, 106610.

Mandowski, A., 2005. On the verification of the simple trap model by simultaneous TL/TSC measurements. Physica B358, 166–173.

McKeever, S.W.S., 1985. Thermoluminescence of Solids. Cambridge University Press, p. 376.

McKeever, S.W.S., Rhodes, J.F., Mathur, V.K., Chen, R., Brown, M.D., Bull, R.K., 1985. Numerical solutions to the rate equations governing the simultaneous release of electrons and holes during thermoluminescence and isothermal decay. Phys. Rev. 32, 3835–3843.

Meisl, N.K., Huntley, D.J., 2005. Anomalous fading parameters and activation energies of feldspars. Ancient TL 23, 1–4.

Merzbacher, E., 1970. Quantum Mechanics. John Wiley, New York.

Messiah, A., 1963. Quantum Mechanics. John Wiley, New York.

Pagonis, V., Jain, M., Murray, A.S., Ankjærgaard, C., Chen, R., 2012. Modeling of the shape of infrared stimulated luminescence signals in feldspars. Radiat. Meas. 47, 870–876.

Pagonis, V., 2019. Recent advances in the theory of quantum tunneling for luminescence phenomena. In: Chen, Reuven, Pagonis, Vasilis (Eds.), Advances in Physics and Applications of Optically and Thermally Stimulated Luminescence. World Scientific, London (Chapter 2).

Pagonis, V., 2021. Luminescence, Data Analysis and Modeling in R. Springer, Cham, Switzerland (Chapter 6).

Polymeris, G.S., Sfampa, L.K., Niora, M., Stefanaki, E.C., Malletzidou, L., Giannoulatou, V., Pagonis, V., Kitis, G., 2018. Anomalous fading in TL, OSL and TA-OSL signals of Durango apatite for various grain size fractions; from micro to nano scale. J. Lumin. 195, 216–224.

Polymeris, G.S., Giannoulatou, V., Paraskevopoulos, K.M., Pagonis, V., Kitis, G., 2022. Anomalous fading in thermoluminescence signal of ten different K-feldspar samples and correlation to structural state characteristics. Radiat. Meas. 155, 106789.

Riedesel, S., Bell, A.M.T., Duller, G.A.T., Finch, A.A., Jain, M., Pearce, N.J., Roberts, H. M., 2021. Exploring sources of variation in thermoluminescence emissions and anomalous fading in alkali feldspars. Radiat. Meas. 141, 106541.

Schulman, J.H., Ginther, S.G., Gorbics, S.G., Nash, A.E., West, E.J., Attix, F.H., 1969. Anomalous fading of CaF_2:Mn TL dosimeters. Appl. Radiat. Isot. 20, 523–527.

Schön, M., 1942. Zum leuchtmechanismus der Kristallphosphore. Z. Phys. 119, 463–472.

Sears, W.R., 1960. Small Perturbations Theory. Princeton University Press, Princeton, New Jersey.

Sfampa, I.K., Polymeris, G.S., Tsirliganis, N.C., Pagonis, V., Kitis, G., 2014. Prompt isothermal decay of thermoluminescence in an apatite exhibiting strong anomalous fading. Nucl. Instrum. Methods Phys. Res. 320, 57–63.

Shenker, D., Chen, R., 1971. Numerical curve fitting of general-order kinetics glow peaks. J. Phys. D Appl. Phys. 4, 287–291.

Stoneham, D., Winter, M.B., 1988. The removal of anomalous fading in authenticity samples. Nucl. Tracks Radiat. Meas. 14, 127–130.

Tsirliganis, N.C., Polymeris, G.S., Kitis, G., Pagonis, V., 2007. Dependence of the anomalous fading of the TL and blue-OSL of fluorapatite on the occupancy of the tunneling recombination sites. J. Lumin. 126, 303–308.

Visocekas, R., Ouchene, M., Gallois, B., 1983. Tunneling afterglow and anomalous fading in dosimetry with $CaSO_4$:Dy. Nucl. Instrum. Methods 214, 553–555.

Visocekas, R., 2000. Monitoring anomalous fading of TL of feldspars by using far-red emission as a gauge. Radiat. Meas. 32, 499–504.

Wintle, A.G., 1973. Anomalous fading of thermoluminescence in mineral samples. Nature 245, 143–144.

Wintle, A.G., 1977. Detailed study of a thermoluminescent mineral exhibiting anomalous fading. J. Lumin. 15, 385–393.